HHS Public Access

Author manuscript

Biochim Biophys Acta. Author manuscript; available in PMC 2017 September 27.

Published in final edited form as:

Biochim Biophys Acta. 2015 September ; 1852(9): 1755–1764. doi:10.1016/j.bbadis.2015.05.006.

Neuraminidase-1 mediates skeletal muscle regeneration

Juliana de Carvalho Neves[a], **Vanessa Rodrigues Rizzato**[a], **Alan Fappi**[a], **Mariana Miranda Garcia**[a], **Gerson Chadi**[a], **Diantha van de Vlekkert**[b], **Alessandra d'Azzo**[b], and **Edmar Zanoteli**[a,*]

[a]Department of Neurology, University of São Paulo, São Paulo, SP Brazil 01246-903

[b]Department of Genetics, St. Jude Children's Research Hospital, Memphis TN, 38105 USA

Abstract

Neuraminidase-1 (NEU1) is the sialidase responsible for the catabolism of sialoglycoconjugates in lysosomes. Congenital NEU1 deficiency causes sialidosis, a severe lysosomal storage disease associated with a broad spectrum of clinical manifestations, which also include skeletal deformities, skeletal muscle hypotonia and weakness. *Neu1*$^{-/-}$ mice, a model of sialidosis, develop an atypical form of muscle degeneration caused by progressive expansion of the connective tissue that infiltrates the muscle bed, leading to fiber degeneration and atrophy. Here we investigated the role of Neu1 in the myogenic process that ensues during muscle regeneration after cardiotoxin-induced injury of limb muscles. A comparative analysis of cardiotoxin-treated muscles from *Neu1*$^{-/-}$ mice and *Neu1*$^{+/+}$ mice showed increased inflammatory and proliferative responses in the absence of Neu1 during the early stages of muscle regeneration. This was accompanied by significant and sequential upregulation of *Pax7*, *MyoD*, and *myogenin* mRNAs. The levels of both MyoD and myogenin proteins decreased during the late stages of regeneration, which most likely reflected an increased rate of degradation of the myogenic factors in the *Neu1*$^{-/-}$ muscle. We also observed a delay in muscle cell differentiation, which was characterized by prolonged expression of embryonic myosin heavy chain, as well as reduced myofiber cross-sectional area. At the end of the regenerative process, collagen type III deposition was increased compared to wild-type muscles and internal controls, indicating the initiation of fibrosis. Overall, these results point to a role of Neu1 throughout muscle regeneration.

Keywords

NEU1; sialidosis; skeletal muscle regeneration; cell proliferation; muscle maturation; fibrosis

[*]Corresponding author: Edmar Zanoteli, Department of Neurology, University of São Paulo, 455 Dr. Arnaldo Ave, Room 2119, São Paulo SP Brazil 01246-903, Telephone: +55 11 30617460, zanoteli@terra.com.br.

1. INTRODUCTION

Neuraminidases catalyze the removal of sialic acid residues from the nonreducing end of glycoproteins, glycolipids, oligosaccharides, and polysaccharides [1]. Four distinct neuraminidases, neuraminidase-1 (NEU1) through NEU4, are found in mammals. These exoglycosidases differ in their subcellular distribution and substrate specificity: NEU1 is lysosomal; NEU2 is cytosolic; NEU3 is found at the plasma membrane, and NEU4 appears to be distributed in lysosomes, mitochondria, and endoplasmic reticulum [2, 3]. In mammalian cells, enzymatically active NEU1 is found in complex with the serine carboxypeptidase protective protein/cathepsin A and β-galactosidase [4, 5]. Association with the former is necessary for NEU1 to be correctly compartmentalized and activated in lysosomes [6].

NEU1 deficiency leads to sialidosis, an autosomal recessive lysosomal storage disease caused by genetic mutations at the *NEU1* locus on chromosome 6p21 [7]. Patients with sialidosis type-I manifest signs of the disease mostly during the second decade of life, including progressive loss of vision with macular degeneration (cherry-red spots), nystagmus, ataxia, seizures, and myoclonus syndrome. Patients with sialidosis type-II suffer a very severe condition, with onset of symptoms at birth or during the early neonatal period and reduced lifespan. Fetal hydrops, neonatal ascites, dysmorphic Hurler-like features, dysostosis multiplex, hepatosplenomegaly, and severe neurologic impairment starting in the perinatal period or infancy are common pathologic manifestations in type-II cases [7, 8]. A subset of patients with sialidosis experiences skeletal deformities, skeletal muscle atrophy and hypotonia [9].

Neu1$^{-/-}$ mice have phenotypic abnormalities intermediate between sialidosis type-I and -II, but they faithfully recapitulate the complex and widespread biochemical and morphological changes characteristic of the human disease [10]. Numerous studies in vitro and in mouse models have implicated NEU1 in fundamental biological processes that go beyond its canonical degradative function; these include immune response and inflammation [11, 12], cell proliferation [13, 14], and tumor cell migration and metastasis [1, 15, 16]. A primary role of NEU1 as a negative regulator of lysosomal exocytosis has been identified [17–20]. This calcium-regulated process, which is present in virtually all cell types, entails the recruitment of selected lysosomes to the cytoskeletal network, followed by their docking at the plasma membrane. Upon calcium influx, lysosomes fuse with the plasma membrane and release their contents extracellularly [21]. NEU1 limits the number of lysosomes that dock at the plasma membrane by processing the sialic acids on the lysosome-associated membrane protein 1 (LAMP1), one of its substrates. Deficiency of NEU1 results in the accumulation of an oversialylated LAMP1, which leads to exacerbated lysosomal exocytosis in many tissues and cell types with deleterious consequences on the integrity of the extracellular matrix and plasma membrane and overall tissue homeostasis.

In the *Neu1*$^{-/-}$ skeletal muscle, excessive exocytosis of lysosomal contents into the extracellular matrix has been linked to the abnormal expansion of connective tissue, which is associated with increased synthesis and deposition of collagen and other of its components due to hyper proliferation of fibroblasts [20]. We found that fibroblasts with exacerbated

lysosomal exocytosis infiltrate the adjacent muscle fibers, which gradually become fragmented, vacuolated, and ultimately degenerate, leading to progressive atrophy [20]. Although we know that myopathy and muscular degeneration are part of the pathogenesis of sialidosis in children and in the mouse model, no one has investigated how myogenesis and muscle regeneration occur in the context of NEU1 deficiency in vivo. However, in vitro studies with C2C12 myoblasts have suggested that NEU1 expression is regulated by transcription factors, like MyoD, that are involved in skeletal muscle regeneration and myogenesis [22, 23]. In addition, NEU1 expression appears to be strictly controlled during the early stages of C2C12 cell differentiation, because Neu1 overexpression during the course of differentiation suppresses myogenin and myosin heavy chain expression, thus disrupting the differentiation process [23].

Cardiotoxin (CTX) injection is among the easiest and most reproducible methodologies to induce muscle regeneration [reviewed in 24]. CTX causes depolarization and disruption of plasma membranes of muscular cells; thus it induces local necrosis and regeneration [24]. Right after muscular damage, neutrophils and macrophages infiltrate the tissues and myogenic precursor cells start to proliferate [24]. Different myogenic regulatory factors (among them MyoD, Myf5, myogenin and MRF4) are successively expressed in the course of muscle regeneration. Furthermore, immature variants of myosins, initially embryonic myosin heavy chain, are progressively substituted by mature forms of myosin (fast and/or slow isoforms). These events stimulate the differentiation of muscle precursor cells, which fuse with themselves and with injured fibers to form new skeletal muscle fibers [24].

Here, we evaluate the course of muscle regeneration after cardiotoxin (CTX)-induced injury of wild-type or *Neu1*$^{-/-}$ muscle and assess the extent of cell proliferation, the inflammatory response, the grade of maturation of myofibers, and the deposition of extracellular matrix at different stages of the regenerative process that occurs after an injury.

2. MATERIAL AND METHODS

2.1. Animals

Male *Neu1*$^{-/-}$ and wild-type (*Neu1*$^{+/+}$) mice (FVB/NJ background), aged 8 weeks, were used in this study. *Neu1*$^{-/-}$ mice were previously generated by targeted disruption in the *Neu1* locus [10]. Animals were housed in the animal facility, under controlled temperature, humidity, and lighting (12-h light/dark cycle). Food and water were provided ad libitum. All procedures in mice were approved by the Animal Care and Use Committee of the School of Medicine of the University of São Paulo and followed NIH guidelines.

2.2. Induction of necrosis and regeneration of muscle

Cardiotoxin (CTX; Sigma) purified from *Naja mossambica mossambica* was used to induce local necrosis after intraperitoneal anesthesia with 5mg/kg of diazepam and 100mg/kg of ketamin. CTX (10 mM) was injected in the proximal tendon region of the right tibialis anterior (TA) muscle toward the distal tendon; the left TA muscle was used as an internal control (CTR). CTX-injected *Neu1*$^{-/-}$ and *Neu1*$^{+/+}$ mice (n = 5 per group) were euthanized at day 1, 3, 5, 7, 10, 14, 21, or 28 after CTX administration. Right TA muscles from

untreated *Neu1*$^{-/-}$ and *Neu1*$^{+/+}$ mice (2 months old, n = 5 per genotype) were used as a control group (day 0). TA muscles were dissected, snap-frozen in isopentane, cooled in liquid nitrogen, and stored at −80 °C until use.

2.3. Histology

Transverse sections (7 μm) of the frozen TA muscles were cut on a cryostat (Leica CM3000). The sections were stained with hematoxylin and eosin (H&E) for overall morphologic assessment and examined under a light microscope (Olympus AX70). Cross-sectional areas of TA fibers were measured using ImageJ software (NIH Software). At least 200 fibers were considered per animal, and the mean fiber area was calculated for each muscle.

2.4. Immunohistochemistry

Frozen sections were thawed, and endogenous peroxidase activity was quenched with 0.3% hydrogen peroxide in phosphate-buffered saline (PBS) for 30 min. The sections were blocked with 1% bovine serum albumin (BSA), 0.5% Tween-20, and 10% normal goat serum in PBS for 1 h and incubated overnight at 4 °C with rat anti-collagen III (1:100 dilution) (ACRIS Pharmaceuticals; BM4018), rat anti-LY6G (1:50 dilution) (BD Biosciences; 553124) and rat anti-CD11b (1:100 dilution) (BD Biosciences; 557395); all antigens were diluted in blocking solution. On the next day, the sections were incubated with biotinylated anti-rat secondary antibody for 1 h at room temperature and then reacted with ABC reagent (Vector Laboratories) for 1 h at room temperature. The sections were incubated with 3,3′-diaminobenzidine substrate for 2 min and then washed in distilled water to stop the reaction. They were then counterstained with hematoxylin and examinated under a light microscope.

2.5. Immunofluorescence microscopy

Frozen sections were fixed in acetone for 20 min and blocked with 2% BSA and 10% normal serum in PBS for 30 min. Sections were incubated with AffiniPure Fab Fragment Goat Anti-Mouse IgG (H+L) (Jackson ImmunoResearch; 115-007-003) in PBS (1:10 dilution) for 1 h at room temperature and incubated overnight at 4 °C with embryonic myosin heavy chain (Developmental Studies Hybridoma Bank) in blocking solution (1:20 dilution). The next day, the sections were blocked for 10 min and incubated with FITC-AffiniPure Goat Anti-Mouse IgG (H+L) (Jackson ImmunoResearch; 115-095-003) in blocking solution (1:200 dilution) for 1 h at room temperature. Slides were mounted with Vectashield mounting medium/DAPI (Vector; H-1200). Control sections were incubated with secondary antibody only. The slides were examined under a fluorescence microscope (Olympus AX70).

2.6. BrdU

Mice euthanized on day 3, 5, or 7 were also injected intraperitoneally with 160 mg/kg 5-bromo-2′-deoxyuridine (BrdU; Sigma). Mice were euthanized 6 h after injection, and the muscles were processed as described in sections 2.3–2.5. For the immunofluorescence staining, an extra step was added to the protocol. A 30-min treatment with 1.5 M HCl at

room temperature prior to incubation with the BrdU primary antibody (1:100 dilution) (Sigma; B8434). The number of $BrdU^+$ nuclei in each muscle was quantified, and the mean was calculated per animal.

2.7. Real-time PCR

Total RNA was isolated using TRIzol Reagent (Life Technologies) and treated with DNAse I (Applied Biosystems/Ambion) according to the manufacturer's instructions. First-strand cDNA was transcribed using 1 μg total RNA with TaqMan Reverse Transcription Reagents (Life Technologies). RT-PCR was executed with Maxima SYBR Green PCR/ROX qPCR Master Mix (Thermo Scientific) on a StepOne Plus machine (Applied Biosystems). The primers used are summarized in Suppl. Table 1. The data obtained were subjected to calculations of relative expression and normalized using *GAPDH* expression.

2.8. Western blotting

For Western blot analysis, TA muscle fragments were homogenized in 5 volumes of RIPA buffer (10% SDS, 70 mMol/L Tris-HCl (pH 6.7), 10 mMol/L EDTA, 5% β-mercaptoethanol, and protease inhibitors (Roche) using a Dounce homogenizer. The homogenates were centrifuged at 13,000×g for 5 min at 4 °C, and the supernatants were transferred to new microtubes. The protein concentrations were determined by absorbance (A = 595) using a BSA solution stardard. Samples (25 μg) were subjected to electrophoresis on SDS-PAGE gels (10% or 12%) and transferred to PVDF membranes. The membranes were blocked with 10% nonfat milk in tris-buffered saline containing 0.05% Tween-20 (TBS/T) for 20 min and incubated with mouse anti-myogenin (Sigma; M5815, 1:2000 dilution) and mouse anti-MyoD (BD Pharmingen; 554130, 1:3000 dilution) overnight at 4 °C. The membranes were washed with TBS/T and incubated with horseradish peroxidase - conjugated goat anti-mouse antibody (1:6000 dilution) for 1 h. They were then incubated with Western Lightning Chemiluminescence Reagent Plus (PerkinElmer Life Science) for 1 min and then developed against X-ray films. Coomassie Brilliant Blue was used to visualize protein loading. The membranes were digitalized, and total protein was quantified using ImageJ 1.43u software.

2.9. Sialic acid assay

Bound sialic acid content was obtained using EnzyChrom Sialic Acid Assay Kit (BioAssay Systems). TA muscle lysates were either treated with a hydrolysis reagent (1 h at 80 °C) for cleavage of bound sialic acid content or used untreated to measure free sialic acid. The samples were placed in black clear - bottom 96-well plates, probed with dye reagent and the enzyme provided by the kit. The amount of sialic acid of the samples was measured in excitation wavelength of 535 nm and emission wavelength of 595 nm, and compared to a 0 to 500 pmol sialic acid standard curve.

2.10. Statistical analyses

Statistical analyses were performed using 2-way ANOVA test followed by either Bonferroni post-test (Gaussian distribution) or Mann-Whitney test (non-Gaussian distribution). The results are presented as means ± standard deviations. Significant variations were accepted

when $p \leq 0.05$. Statistical analyses were performed using GraphPad Prism 5 software for Windows (GraphPad Software).

3. RESULTS

3.1. Neu1 expression is upregulated during the early stages of muscle regeneration

We first assessed the pattern of *Neu1* mRNA expression during muscle regeneration after local CTX injection into $Neu1^{+/+}$ TA muscles by using RT-qPCR. *Neu1* expression was significantly increased at day 1 after injury and remained highly expressed until day 10. Normal expression levels resumed at day 14, indicating that *Neu1* is upregulated mainly during the first stages of muscle regeneration (Fig. 1).

3.2. Neu1$^{-/-}$ muscles have higher content of bound sialic acid

Neu1 upregulation during regeneration, as well previous data about the effects of Neu1 deficiency in skeletal muscles [20], lead to the hypothesis that Neu1 activity is important for the normal physiology of this tissue. In order to verify the sialylation patternin skeletal muscles, we compared the amount of bound sialic acid in $Neu1^{+/+}$ and $Neu1^{-/-}$ in TA muscles, confirming an increase of sialylation in $Neu1^{-/-}$ muscles (Fig. 2).

3.3. CTX-injured Neu1$^{-/-}$ skeletal muscle displays a dystrophic phenotype at the end of the regeneration process

The myofiber areas of the $Neu1^{-/-}$ TA muscle were, in general, smaller than those of the $Neu1^{+/+}$ TA muscle at all time points after CTX injection (Fig. 3). In fact, the $Neu1^{+/+}$ myofibers regained their normal size before or around day 28 of regeneration, whereas the $Neu1^{-/-}$ myofibers remained smaller at the end of the recovery period (Fig. 3), indicating an impaired or delayed regeneration process (or trophism) of the $Neu1^{-/-}$ muscle.

To determine whether any morphologic changes occurred after CTX injection and whether those changes differed in the $Neu1^{-/-}$ versus $Neu1^{+/+}$ muscles, we examined cross sections of the injured muscles stained with H&E (Fig. 4). After the CTX injection, both $Neu1^{+/+}$ and $Neu1^{-/-}$ TA muscles showed widespread damage of the fibers. During the first 3 days posttreatment, the muscles showed areas with prominent necrosis (pale and fragmented cytosol) and increased cellularity (Fig. 4). After day 5, the $Neu1^{+/+}$ TA muscle exhibited small, round, regenerative muscle fibers with centralized nuclei (myotubular aspect). The excessive connective tissue seen at day 3 was replaced by growing, newly formed myofibers at day 7 (Fig. 4). Full histologic reorganization in the injured $Neu1^{+/+}$ muscle occurred between day 14 and day 28 (Fig. 4). In contrast, $Neu1^{-/-}$ muscle showed expanded endomysium and perimysium spaces (connective tissue) throughout the regeneration period. Immunostaining for collagen III at day 14 showed increased expression of this collagen in the endomysium space (Fig. 5A). Collagen III levels remained high in the $Neu1^{-/-}$ regenerated muscle but were normalized around day 21 in the $Neu1^{+/+}$ muscle (Fig. 5A). Although some regions of the regenerating $Neu1^{+/+}$ muscle had an increased number of fibroblasts, similar areas in the $Neu1^{-/-}$ muscle displayed a dramatic expansion of the connective tissue with increased cellularity at day 28 (Fig. 5B).

3.4. The expression of MyoD and myogenin is altered and myofiber maturation is delayed in Neu1$^{-/-}$ muscle during regeneration

We next evaluated the mRNA and protein expressions of MyoD and myogenin to determine whether the Neu1 deficiency influenced muscle maturation in earlier and later stages of skeletal muscle regeneration. In *Neu1*$^{+/+}$ muscle, *MyoD* mRNA expression peaked at day 3 after injury and rapidly diminished from day 5 onward (Fig. 6A). *MyoD* mRNA had a similar expression profile in CTX-injured *Neu1*$^{-/-}$ muscle, but its expression levels were significantly higher than in *Neu1*$^{+/+}$ muscle from day 3 to day 7 (Fig. 6A). In contrast, the level of MyoD protein was significantly lower in *Neu1*$^{-/-}$ muscle at day 5 and day 7 than it was in *Neu1*$^{+/+}$ muscle, which remained high until day 7 (Fig. 6B). From day 7 on, MyoD levels were very low in all groups and statiscally equal to day 0 in both genotypes. There were no differences between MyoD expression in *Neu1*$^{+/+}$ and *Neu1*$^{-/-}$ muscles (Suppl. Fig. 1).

As expected, *myogenin* mRNA levels in injured *Neu1*$^{+/+}$ muscle peaked at day 7 and day 14, about 3 days later than *MyoD*, and the protein was still overexpressed at day 21 (Figs. 6C–D). *Myogenin* mRNA levels were significantly higher in *Neu1*$^{-/-}$ muscle than in the *Neu1*$^{+/+}$ muscle only at day 7 but declined to the levels of the *Neu1*$^{+/+}$ muscle at day 14 and day 21 (Fig. 6C). Similarly to MyoD, myogenin protein levels were reduced at day 7, a time when *myogenin* mRNA levels were the highest (Fig. 6D). These results suggest that these myogenic transcription factors degrade faster during the early stages of *Neu1*$^{-/-}$ muscle regeneration.

The expression of transcription factors can directly influence the levels of muscle-specific proteins; therefore, we also investigated the expression of embryonic myosin heavy chain via indirect immunofluorescence. Embryonic myosin heavy chain was expressed at high levels in both groups of CTX-injured muscles at day 5 of regeneration. Nevertheless, the highest expression of embryonic myosin heavy chain occurred in the *Neu1*$^{-/-}$ muscle and persisted for a longer period after injury, especially in smaller fibers, which indicated a delay in the maturation of the myofibers (Fig. 7).

3.5. Atrogin-1 and MuRF-1 genes are upregulated at days 5 and 7 of muscle regeneration in Neu1$^{-/-}$ muscles

Because of discrepancies between gene and protein expression in *Neu1*$^{-/-}$ muscles, we reasoned that protein degradation could be occurring. The ubiquitin-proteasome system is an important mechanism to degrade proteins in skeletal muscles. This system requires the interaction of three enzimes (E1, E2 and E3) to cause the ubiquitination of proteins, and its subsequent degradation [25]. Atrogin-1 and MuRF-1 are the mostly encoded E3 ligases when the ubiquitin-proteasome system is active in muscles [26, 27]. For this reason, we decided study gene expression of *atrogin-1* and *MuRF-1*. In normal mice, *atrogin-1* and *MurF-1* are upregulated at day 7; in *Neu1*$^{-/-}$ muscles, both atrogenes were upregulated at days 5 and 7 of skeletal muscle regeneration. Moreover, these genes are overexpressed in Neu1 deficient muscles, when compared to wild-type muscles (Fig. 8).

3.6. Abnormally increased cell proliferation in CTX-injured Neu1$^{-/-}$ skeletal muscles

We next assessed the influence of Neu1 deficiency on cell proliferation by monitoring BrdU incorporation at days 3, 5, and 7 of skeletal muscle regeneration (Fig. 9A). Although the pattern of proliferation was similar between *Neu1*$^{-/-}$ and *Neu1*$^{+/+}$ muscles, the number of BrdU^{+} nuclei was significantly higher in the *Neu1*$^{-/-}$ muscle at day 5 and day 7 (Fig. 9A). This result suggests that deficiency of Neu1 affects the proliferative status of cells during the early stages of muscle regeneration.

Considering that different cell types (e.g., satellite and inflammatory cells) are recruited or activated at the site of injury during early regeneration, we tested the expression of *Pax7*, a marker of satellite cells, between day 0 and day 7. The expression of *Pax7 was* higher in the injured *Neu1*$^{-/-}$ muscle than in the control muscle throughout the course of the experiments (Fig. 9B). These findings suggest that the increased cell proliferation in the *Neu1*$^{-/-}$ muscle after injury can be contributed to not only fibroblasts but also satellite cells.

3.7. Inflammatory response is disturbed in CTX-injured Neu1$^{-/-}$ muscle

We analyzed the inflammatory response to CTX-induced injury by immunohistochemical staining of neutrophils and macrophages. In *Neu1*$^{-/-}$ and *Neu1*$^{+/+}$ muscles, the neutrophils was comparable until day 3 after injury (Fig. 10A). At day 5, a few neutrophils remained at the site of injection in the *Neu1*$^{+/+}$ muscles, but they were no longer detected at day 10. In the *Neu1*$^{-/-}$ skeletal muscle, neutrophils were no longer present by day 5 (Fig. 10A), which indicated a reduced neutrophilic response in the *Neu1*$^{-/-}$ mice.

Macrophage infiltration was detected from day 1 to day 10 after CTX-induced injury (Fig. 10B). However, in the *Neu1*$^{+/+}$ muscle the highest number of CD11b^{+} cells was seen at day 5 and declined at day 10. In contrast, in the *Neu1*$^{-/-}$ muscle an increased number of macrophages was seen until day 10 (Fig. 10B), suggesting a prolonged inflammatory response in the *Neu1*$^{-/-}$ muscles.

The analysis of *CD11b* mRNA confirmed higher expression of this marker in the *Neu1*$^{-/-}$ skeletal muscle throughout the regeneration period (Fig. 10C). The peak of *CD11b* expression was around day 3, and expression returned to normal levels about day 10 in both groups.

4. DISCUSSION

In a previous study with 11 patients with sialidosis, mutant Neu1 residual activity was related with the clinical severity of the disease [9]. This study included two patients with muscular commitment; both of them had nucleic acid substitutions in exons 4 and 5, resulting in single amino acid substitutions (Arg294Ser in patients 1 and 2; Leu231His in patient 1, and Gly218Ala in patient 2). This study also described that sialidosis has different degrees of penetrance [9], what could explain why only a subset of patients present muscular symptoms. It is not possible to characterize histologically and molecularly the skeletal muscle of patients with sialidosis, because no biopsy has been obtained so far. This reality reinforces the importance of our animal model to understand muscle physiology in different situations.

The aim of this study was to determine the effect of Neu1 deficiency on skeletal muscle regeneration in vivo after CTX injection. Overall, our findings indicated that losing Neu1 function affects important aspects of skeletal muscle regeneration, including the inflammatory response, myofiber maturation, and extracellular matrix reconstitution. Although the molecular mechanisms underlying the altered regenerative process in the Neu1-deficient mice are still under investigation, the results of this study reiterate the importance of controlling the sialic acid content of target NEU1 substrates for skeletal muscle physiology [20].

Here we showed that Neu1 deficiency is associated with the expansion of the perimysium and endomysial spaces during skeletal muscle regeneration, resulting in a dystrophic phenotype. In skeletal muscle, the interplay between the extracellular matrix and individual muscle fibers is crucial for the normal function and integrity of the tissue. In addition to providing mechanical support, the extracellular matrix and the basement membrane/basal lamina, in particular, function as a scaffold during muscle regeneration. Disturbing any of these components may adversely affect muscle strength and integrity and result in muscle disease or defective skeletal muscle regeneration [28, 29]. In *Neu1*$^{-/-}$ mice, muscle tissue undergoes progressive degeneration that is associated with profound alterations in the extracellular matrix components and infiltration of the muscle bed by connective tissue [20]. Many of these abnormalities can be attributed to increased proliferation of fibroblast-like cells, abnormal deposition of collagen fibers, and enhanced proteolytic activity in the extracellular matrix. These features are linked, at least in part, to excessive Neu1-dependent lysosomal exocytosis [17, 20].

LAMP1, a substrate of Neu1, is important for the docking of lysosomes to the PM [17]. In the absence of Neu1, oversialylated LAMP1 has a longer half-life, and this increases the number of lysosomes poised to dock at the PM and engage in lysosomal exocytosis [17]. The downstream effect is the enhanced release of catalytically active proteases and glycosidases extracellularly, a phenomenon that affects the processing of cell-surface proteins and extracellular matrix components [17]. These authors also demonstrated an inverse correlation between the levels of residual NEU1 activity and lysosomal exocytosis in fibroblasts of patients with sialidosis and different clinical phenotypes. This feature is fully recapitulated in mouse fibroblasts isolated from *Neu1*$^{-/-}$ skeletal muscle, indicating the involvement of this aberrant process in the development of the muscle phenotype [20].

In this study, we showed that in addition to basal muscular atrophy, regenerating *Neu1*$^{-/-}$ muscle fibers have an impaired growth rate, maintaining a higher degree of atrophy than that of the uninjured *Neu1*$^{-/-}$ muscle fibers, especially during the late stages of muscle regeneration. We previously showed an increased release of cathepsins via lysosomal exocytosis into the extracellular matrix of the *Neu1*$^{-/-}$ muscle connective tissue and activation of matrix metalloproteinases [20]. Both of these events contribute to the atrophic phenotype in the Neu1-deficient muscle and may explain the muscle hypotonia in patients with sialidosis.

In the regenerating *Neu1*$^{-/-}$ muscle fibers, embryonic myosin heavy chain was expressed during the later stages of regeneration, suggesting delayed maturation. In addition, the

expression of myogenic factors (MyoD and myogenin) was abnormal in the *Neu1*$^{-/-}$ regenerating muscle, which indicated that Neu1 deficiency induces changes in the expression profiles of myogenic transcription factors during muscle regeneration. A previous study in C2C12 myoblasts in vitro suggested the involvement of Neu1 in the early stages of myogenesis, possibly under the regulation of MyoD [23]. The authors also showed that in the C2C12 myoblasts the activity of Neu1 is highly and temporally regulated during myogenesis. They postulated that increased Neu1 expression in myoblasts results in the desialylation of surface molecules, leading to the inhibition of differentiation and cell fusion with reduced expression of myogenin and myosins [23]. In agreement with these in vitro studies, we now show that in wild-type mice the expression of *Neu1* was high from day 1 to day 10 after CTX-induced injury.

Usually, skeletal muscle is able to adapt to several physiological conditions through cell and protein turnover [30]. *Atrogin-1* and *MuRF-1* are very important genes that participate in this process [26, 27], but we found that these genes were upregulated at days 5 and 7 of regeneration in *Neu1*$^{-/-}$ muscles, compared to normal muscles. Indeed, atrogin-1 is recognized as the E3 ligase responsible for MyoD degradation [31], what could explain the low levels of MyoD in these mice, even with upregulated gene. Increased expression of *atrogin-1* and reduced expression of *myogenin* had previously been linked to a model of skeletal muscle atrophy [32]. In turn, MuRF-1 controls the half-life of important structural muscle proteins [33–35], including myosin heavy chains [33, 34].

Neu1 is involved in cell proliferation [15]. In arterial smooth muscle cells, Neu1 alters the cellular responsiveness to mitogenic ligands and is a negative regulator of cell proliferation. We have shown that Neu1 regulates fibroblast proliferation and thus extracellular matrix remodeling in skeletal muscle most likely via increased lysosomal exocytosis [20]. Results from our BrdU experiment indicated that Neu1 deficiency increases cell proliferation during skeletal muscle regeneration. We propose that not only fibroblasts but also satellite cells are affected, considering the increased expression of *Pax7*.

Inflammatory process is an important step during muscle regeneration [24], thus we tested neutrophil and macrophage responses at different times after muscle injury. We noticed that the neutrophil response in Neu1-deficient muscle was reduced than that in wild-type muscle at day 3 after injury, and the macrophage response persisted later than day 10. These findings indicate that Neu1 deficiency affects the inflammatory response after muscle injury. Besides, studies have demonstrated the involvement of the sialic acid and NEU1 activity in the regulation of the inflammatory response [36, 37].

Normally, the inflammatory response following muscle injury initiates with the recruitment of neutrophils, which scavenge dead cells and are found in injury sites only a few hours after injury [24, 38, 39]. About 24 h after injury, macrophages are attracted to the site of the injury by proinflammatory neutrophils [24, 38, 39]. Macrophages are the responsible to eliminate cell debris and begin the myogenic process [24]. Oversialylation in plasma membrane receptors appears to affect the adhesion and migration of neutrophils [36]. This feature indicates the possible mechanism related to the diminished neutrophilic reaction we observed. In turn, oversialylation reduces macrophagic phagocytic capacity [37]. The

persistence of these cells at the injury sites we found would compensate the phagocytic defect and ensure downstream events in regeneration [40].

Our findings suggest that Neu1 is important for normal muscle regeneration. Additional studies are needed to elucidate the physiological processes in muscle that depend on the correct expression of NEU1 and may further clarify the involvement of lysosomes and the metabolism of sialic acid in the pathophysiology of muscle diseases.

Supplementary Material

Refer to Web version on PubMed Central for supplementary material.

Acknowledgments

The authors thank Prof. Dr. Chin Jia Lin, Dr. Kátia Cândido Carvalho and colleagues, and Dr. Jessica Ruivo Maximino for assistance. This work was sponsored by *Fundação de Amparo à Pesquisa do Estado de São Paulo* grants 2009/02937-4 and 2011/03853-9 and, in part, by NIH grants GM60950 and DK52025, the Assisi Foundation of Memphis, and ALSAC. A.d'A. holds the Jeweler's Charity Fund Endowed Chair in Genetics and Gene Therapy.

Abbreviations

ANOVA	analysis of variance
BrdU	5-bromo-2′-deoxyuridine
CTX	cardiotoxin
GAPDH	glyceraldehyde 3-phosphate dehydrogenase
H&E	hematoxylin and eosin
LAMP1	lysosome-associated membrane protein 1
NEU1	neuraminidase-1
TA	tibialis anterior muscle

References

1. Monti E, Bonten E, D'Azzo A, Bresciani R, Venerando B, Borsani G, Schauer R, Tettamanti G. Sialidases in vertebrates: a family of enzymes tailored for several cell functions. Adv Carbohydr Chem Biochem. 2010; 64:403–479. [PubMed: 20837202]
2. Miyagi T, Yamaguchi K. Mammalian sialidases: physiological and pathological roles in cellular functions. Glycobiology. 2012; 22:880–896. [PubMed: 22377912]
3. Fanzani A, Zanola A, Faggi F, Papini N, Venerando B, Tettamanti G, Sampaolesi M, Monti E. Implications for the mammalian sialidases in the physiopathology of skeletal muscle. Skelet Muscle. 2012; 2:23. [PubMed: 23114189]
4. Bonten E, van der Spoel A, Fornerod M, Grosveld G, d'Azzo A. Characterization of human lysosomal neuraminidase defines the molecular basis of the metabolic storage disorder sialidosis. Genes Dev. 1996; 10:3156–3169. [PubMed: 8985184]
5. Bonten EJ, Campos Y, Zaitsev V, Nourse A, Waddell B, Lewis W, Taylor G, d'Azzo A. Heterodimerization of the sialidase NEU1 with the chaperone protective protein/cathepsin A prevents its premature oligomerization. J Biol Chem. 2009; 284:28430–28441. [PubMed: 19666471]

6. van der Spoel A, Bonten E, d'Azzo A. Transport of human lysosomal neuraminidase to mature lysosomes requires protective protein/cathepsin A. EMBO J. 1998; 17:1588–1597. [PubMed: 9501080]
7. Thomas GH. Disorders of glycoprotein degradation and structure: α-mannosidosis, β-mannosidosis, fucosidosis and sialidosis. The Metabolic and Molecular Bases of Inherited Disease. 2001:3507–3534.
8. Lowden JA, O'Brien JS. Sialidosis: a review of human neuraminidase deficiency. Am J Hum Genet. 1979; 31:1–18. [PubMed: 107795]
9. Bonten EJ, Arts WF, Beck M, Covanis A, Donati MA, Parini R, Zammarchi E, d'Azzo A. Novel mutations in lysosomal neuraminidase identify functional domains and determine clinical severity in sialidosis. Hum Mol Genet. 2000; 9:2715–2725. [PubMed: 11063730]
10. de Geest N, Bonten E, Mann L, de Sousa-Hitzler J, Hahn C, d'Azzo A. Systemic and neurologic abnormalities distinguish the lysosomal disorders sialidosis and galactosialidosis in mice. Hum Mol Genet. 2002; 11:1455–1464. [PubMed: 12023988]
11. Nan X, Carubelli I, Stamatos NM. Sialidase expression in activated human T lymphocytes influences production of IFN-gamma. J Leukoc Biol. 2007; 81:284–296. [PubMed: 17028199]
12. Feng C, Zhang L, Almulki L, Faez S, Whitford M, Hafezi-Moghadam A, Cross AS. Endogenous PMN sialidase activity exposes activation epitope on CD11b/CD18 which enhances its binding interaction with ICAM-1. J Leukoc Biol. 2011; 90:313–321. [PubMed: 21551251]
13. Hinek A, Bodnaruk TD, Bunda S, Wang Y, Liu K. Neuraminidase-1, a subunit of the cell surface elastin receptor, desialylates and functionally inactivates adjacent receptors interacting with the mitogenic growth factors PDGF-BB and IGF-2. Am J Pathol. 2008; 173:1042–1056. [PubMed: 18772331]
14. Arabkhari M, Bunda S, Wang Y, Wang A, Pshezhetsky AV, Hinek A. Desialylation of insulin receptors and IGF-1 receptors by neuraminidase-1 controls the net proliferative response of L6 myoblasts to insulin. Glycobiology. 2010; 20:603–616. [PubMed: 20100694]
15. Uemura T, Shiozaki K, Yamaguchi K, Miyazaki S, Satomi S, Kato K, Sakuraba H, Miyagi T. Contribution of sialidase NEU1 to suppression of metastasis of human colon cancer cells through desialylation of integrin beta4. Oncogene. 2009; 28:1218–1229. [PubMed: 19151752]
16. Tringali C, Anastasia L, Papini N, Bianchi A, Ronzoni L, Cappellini MD, Monti E, Tettamanti G, Venerando B. Modification of sialidase levels and sialoglycoconjugate pattern during erythroid and erytroleukemic cell differentiation. Glycoconj J. 2007; 24:67–79. [PubMed: 17139558]
17. Yogalingam G, Bonten EJ, van de Vlekkert D, Hu H, Moshiach S, Connell SA, d'Azzo A. Neuraminidase 1 is a negative regulator of lysosomal exocytosis. Dev Cell. 2008; 15:74–86. [PubMed: 18606142]
18. Wu X, Steigelman KA, Bonten E, Hu H, He W, Ren T, Zuo J, d'Azzo A. Vacuolization and alterations of lysosomal membrane proteins in cochlear marginal cells contribute to hearing loss in neuraminidase 1-deficient mice. Biochim Biophys Acta. 2010; 1802:259–268. [PubMed: 19857571]
19. Annunziata I, Patterson A, Helton D, Hu H, Moshiach S, Gomero E, Nixon R, d'Azzo A. Lysosomal NEU1 deficiency affects amyloid precursor protein levels and amyloid-beta secretion via deregulated lysosomal exocytosis. Nat Commun. 2013; 4:2734. [PubMed: 24225533]
20. Zanoteli E, van de Vlekkert D, Bonten EJ, Hu H, Mann L, Gomero EM, Harris AJ, Ghersi G, d'Azzo A. Muscle degeneration in neuraminidase 1-deficient mice results from infiltration of the muscle fibers by expanded connective tissue. Biochim Biophys Acta. 2010; 1802:659–672. [PubMed: 20388541]
21. Jaiswal JK, Andrews NW, Simon SM. Membrane proximal lysosomes are the major vesicles responsible for calcium-dependent exocytosis in nonsecretory cells. J Cell Biol. 2002; 159:625–635. [PubMed: 12438417]
22. Champigny MJ, Johnson M, Igdoura SA. Characterization of the mouse lysosomal sialidase promoter. Gene. 2003; 319:177–187. [PubMed: 14597183]
23. Champigny MJ, Perry R, Rudnicki M, Igdoura SA. Overexpression of MyoD-inducible lysosomal sialidase (neu1) inhibits myogenesis in C2C12 cells. Exp Cell Res. 2005; 311:157–166. [PubMed: 16216242]

24. Charge SB, Rudnicki MA. Cellular and molecular regulation of muscle regeneration. Physiol Rev. 2004; 84:209–238. [PubMed: 14715915]
25. Bonaldo P, Sandri M. Cellular and molecular mechanisms of muscle atrophy. Dis Model Mech. 2013; 6:25–39. [PubMed: 23268536]
26. Bodine SC, Latres E, Baumhueter S, Lai VK, Nunez L, Clarke BA, Poueymirou WT, Panaro FJ, Na E, Dharmarajan K, Pan ZQ, Valenzuela DM, DeChiara TM, Stitt TN, Yancopoulos GD, Glass DJ. Identification of ubiquitin ligases required for skeletal muscle atrophy. Science. 2001; 294:1704–1708. [PubMed: 11679633]
27. Gomes MD, Lecker SH, Jagoe RT, Navon A, Goldberg AL. Atrogin-1, a muscle-specific F-box protein highly expressed during muscle atrophy. Proc Natl Acad Sci U S A. 2001; 98:14440–14445. [PubMed: 11717410]
28. Sanes JR. The basement membrane/basal lamina of skeletal muscle. J Biol Chem. 2003; 278:12601–12604. [PubMed: 12556454]
29. Canty EG, Kadler KE. Procollagen trafficking, processing and fibrillogenesis. J Cell Sci. 2005; 118:1341–1353. [PubMed: 15788652]
30. Sartorelli V, Fulco M. Molecular and cellular determinants of skeletal muscle atrophy and hypertrophy. Sci STKE. 2004; 2004:re11. [PubMed: 15292521]
31. Tintignac LA, Lagirand J, Batonnet S, Sirri V, Leibovitch MP, Leibovitch SA. Degradation of MyoD mediated by the SCF (MAFbx) ubiquitin ligase. J Biol Chem. 2005; 280:2847–2856. [PubMed: 15531760]
32. Fappi A, Godoy TS, Maximino JR, Rizzato VR, de Neves JC, Chadi G, Zanoteli E. The effects of omega-3 fatty acid supplementation on dexamethasone-induced muscle atrophy. Biomed Res Int. 2014; 2014:961438. [PubMed: 24982916]
33. Clarke BA, Drujan D, Willis MS, Murphy LO, Corpina RA, Burova E, Rakhilin SV, Stitt TN, Patterson C, Latres E, Glass DJ. The E3 Ligase MuRF1 degrades myosin heavy chain protein in dexamethasone-treated skeletal muscle. Cell Metab. 2007; 6:376–385. [PubMed: 17983583]
34. Fielitz J, Kim MS, Shelton JM, Latif S, Spencer JA, Glass DJ, Richardson JA, Bassel-Duby R, Olson EN. Myosin accumulation and striated muscle myopathy result from the loss of muscle RING finger 1 and 3. J Clin Invest. 2007; 117:2486–2495. [PubMed: 17786241]
35. Cohen S, Zhai B, Gygi SP, Goldberg AL. Ubiquitylation by Trim32 causes coupled loss of desmin, Z-bands, and thin filaments in muscle atrophy. J Cell Biol. 2012; 198:575–589. [PubMed: 22908310]
36. Cross AS, Sakarya S, Rifat S, Held TK, Drysdale BE, Grange PA, Cassels FJ, Wang LX, Stamatos N, Farese A, Casey D, Powell J, Bhattacharjee AK, Kleinberg M, Goldblum SE. Recruitment of murine neutrophils in vivo through endogenous sialidase activity. J Biol Chem. 2003; 278:4112–4120. [PubMed: 12446694]
37. Seyrantepe V, Iannello A, Liang F, Kanshin E, Jayanth P, Samarani S, Szewczuk MR, Ahmad A, Pshezhetsky AV. Regulation of phagocytosis in macrophages by neuraminidase 1. J Biol Chem. 2010; 285:206–215. [PubMed: 19889639]
38. Couteaux R, Mira JC, d'Albis A. Regeneration of muscles after cardiotoxin injury. I. Cytological aspects. Biol Cell. 1988; 62:171–182. [PubMed: 3390626]
39. Tidball JG. Inflammatory processes in muscle injury and repair. Am J Physiol Regul Integr Comp Physiol. 2005; 288:R345–353. [PubMed: 15637171]
40. Tidball, JG. Inflammation in skeletal muscle regeneration. In: Schiaffino, S., Partridge, T., editors. Skeletal muscle repair and regeneration. Springer; Dordrecht: 2008. p. 243-268.

Highlights

- Deficiency of Neu1 disturbs different stages of skeletal muscle regeneration.
- *Neu1*$^{-/-}$ muscles presented increased inflammatory and proliferative responses during regeneration.
- mRNA and protein levels of muscle specific transcriptions factors were deregulated in *Neu1*$^{-/-}$ muscles.
- *Neu1*$^{-/-}$ muscles had delayed cell differentiation and initiation of fibrotic process.

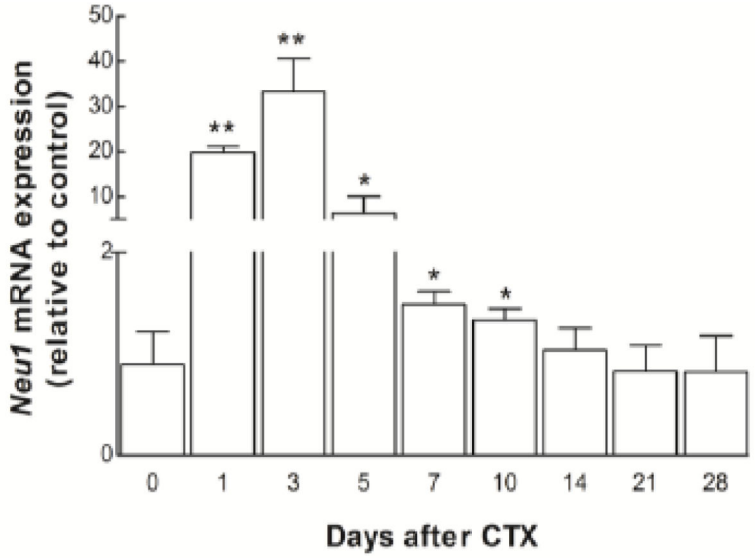

Fig. 1.

Neu1 mRNA expression is temporally regulated during skeletal muscle regeneration after CTX-induced injury. **p* <*0.05* and ***p* <*0.01* indicate differences in the level of *Neu1* expression in regenerating muscle compared to that in untreated control muscle (day 0); Mann-Whitney test (n=5).

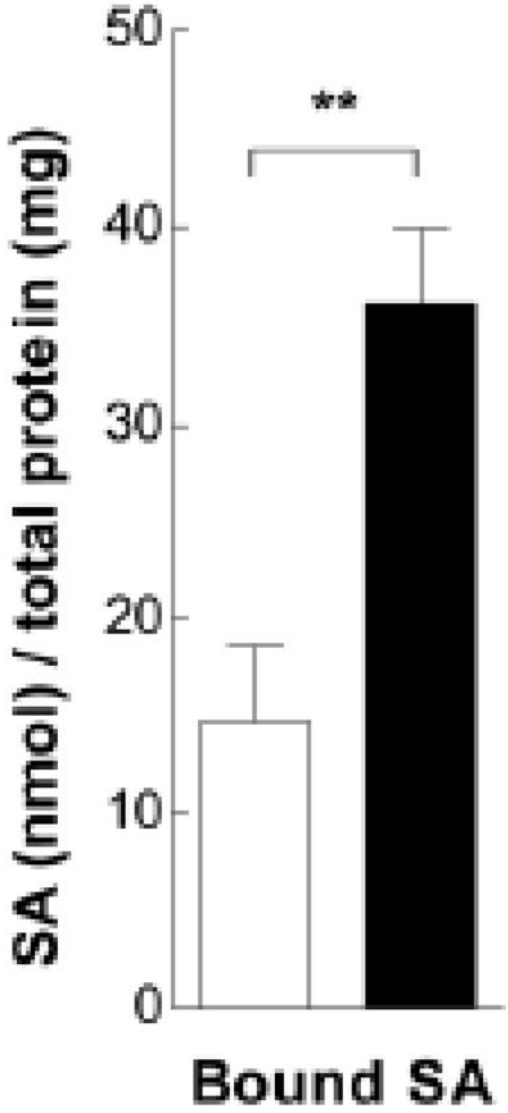

Fig. 2.

Bound sialic acid content in TA muscles. ** $p < 0.01$ indicate differences in the amount of bound sialic acid in $Neu1^{+/+}$ and $Neu1^{-/-}$; Mann-Whitney test (n=3).

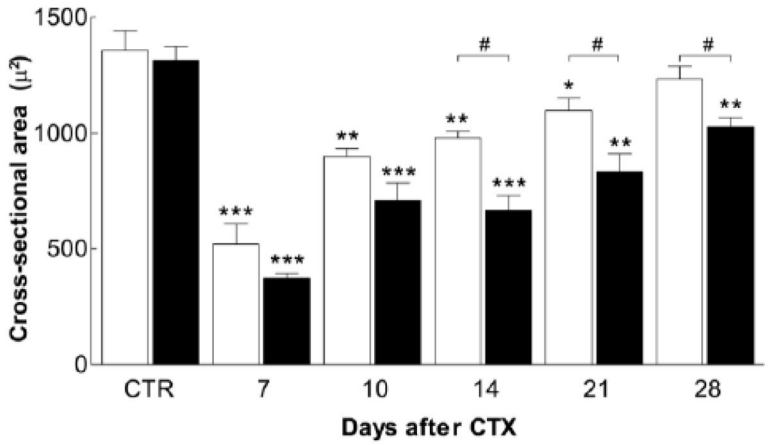

Fig. 3.

The cross-sectional area of myofibers from *Neu1*$^{+/+}$ (white bars) or *Neu1*$^{-/-}$ (black bars) muscles during regeneration after CTX-induced injury. *$p < 0.05$, **$p < 0.01$, and ***$p < 0.001$ indicate differences in the cross-sectional area of myofibers in regenerating muscles compared with that in untreated control muscle (CTR); #$p < 0.05$ indicates differences between the cross-sectional area of *Neu1*$^{-/-}$ myofibers and that of *Neu1*$^{+/+}$ myofibers on the same day of regeneration; two-way ANOVA with Bonferroni post-test (n=5).

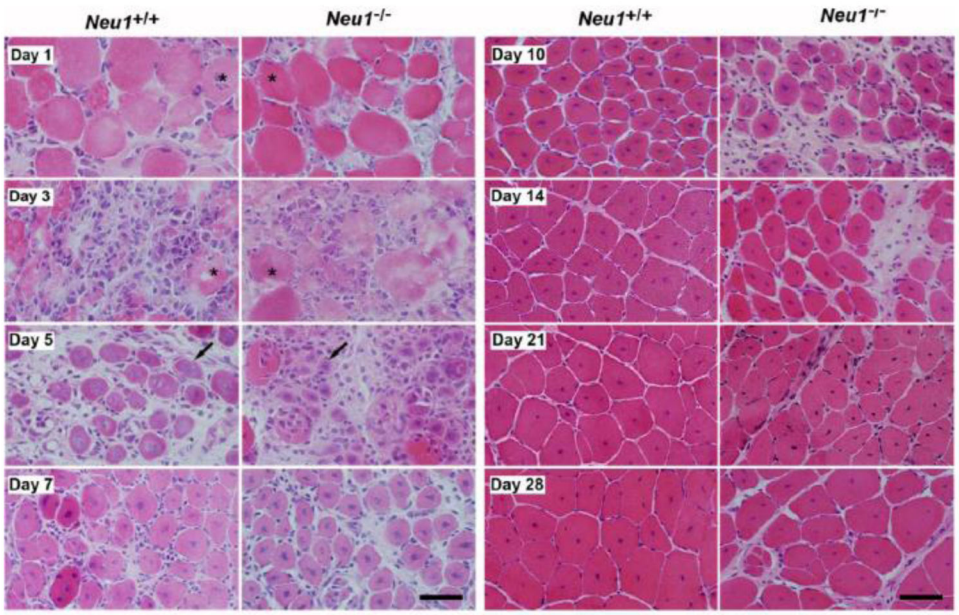

Fig. 4.

H&E staining of transverse sections of *Neu1*$^{+/+}$ and *Neu1*$^{-/-}$ TA muscles during regeneration after CTX-induced injury (n=5). Degenerating fibers (asterisks) are noted, especially on days 1 and 3 postinjection, and regenerative fibers with centralized nuclei (arrows) arise on day 5. A delay in muscle reorganization is noted in the *Neu1*$^{-/-}$ mice, with excessive deposition of extracellular matrix components and smaller muscle fibers. Scale bars = 40 μm and apply to all images.

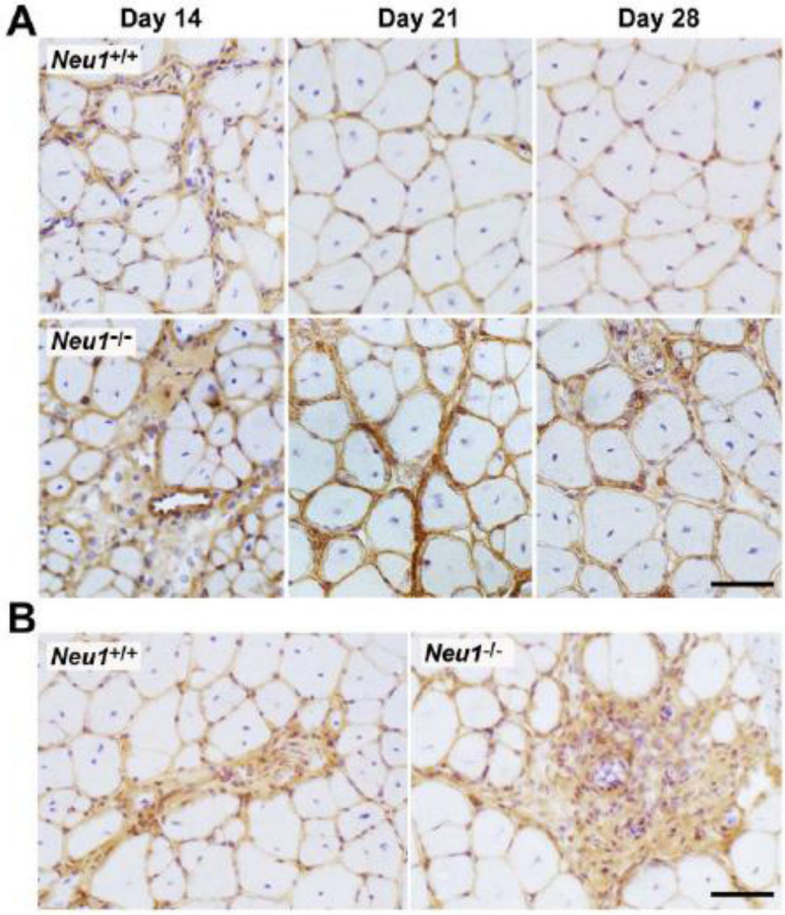

Fig. 5.

Immunohistochemical staining for collagen III in *Neu1*$^{+/+}$ and *Neu1*$^{-/-}$ TA muscles during late stages of regeneration (n=5). Labeling was more intense after day 14 in *Neu1*$^{-/-}$ muscles (A), and greater fibroblast infiltrates can be seen in these mice on day 28 (B). Scale bar = 100 μm and applies to all images.

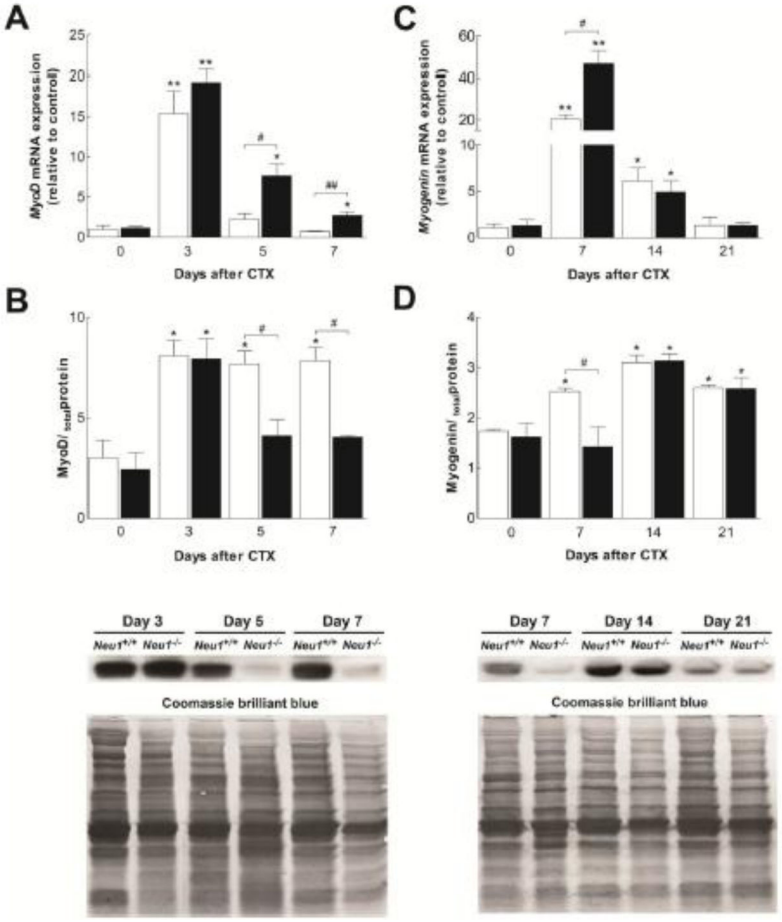

Fig. 6.

The expression of MyoD and myogenin mRNA (A and C) and proteins (B and D) during skeletal muscle regeneration in *Neu1*$^{+/+}$ (white bars) and *Neu1*$^{-/-}$ (black bars) mice. Western blots of MyoD (45 kDa) and myogenin (25 kDa) represent the experimental groups of both genotypes (n=5). *$p < 0.05$ and **$p < 0.01$ indicate differences in the level of expression compared with that in the untreated control muscle (day 0); #$p < 0.05$ and ##$p < 0.01$ indicate differences between the level of mRNA or protein expression in *Neu1*$^{-/-}$ muscle and that in *Neu1*$^{+/+}$ muscle on the same day of regeneration; Mann-Whitney test (n=5).

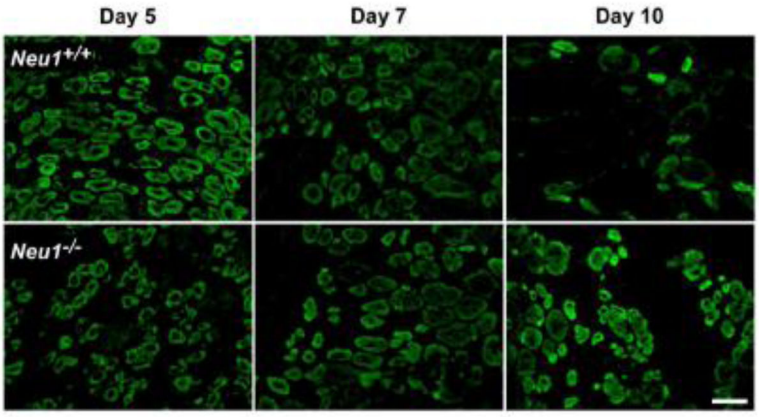

Fig. 7.

Indirect immunofluorescence of embryonic myosin heavy chain in *Neu1*$^{+/+}$ or *Neu1*$^{-/-}$ muscles during regeneration after CTX-induced injury (n=5). The expression of embryonic myosin heavy chain persisted longer in *Neu1*$^{-/-}$ muscles, especially in fibers with a smaller diameter. Scale bar = 40 μm and applies to all images.

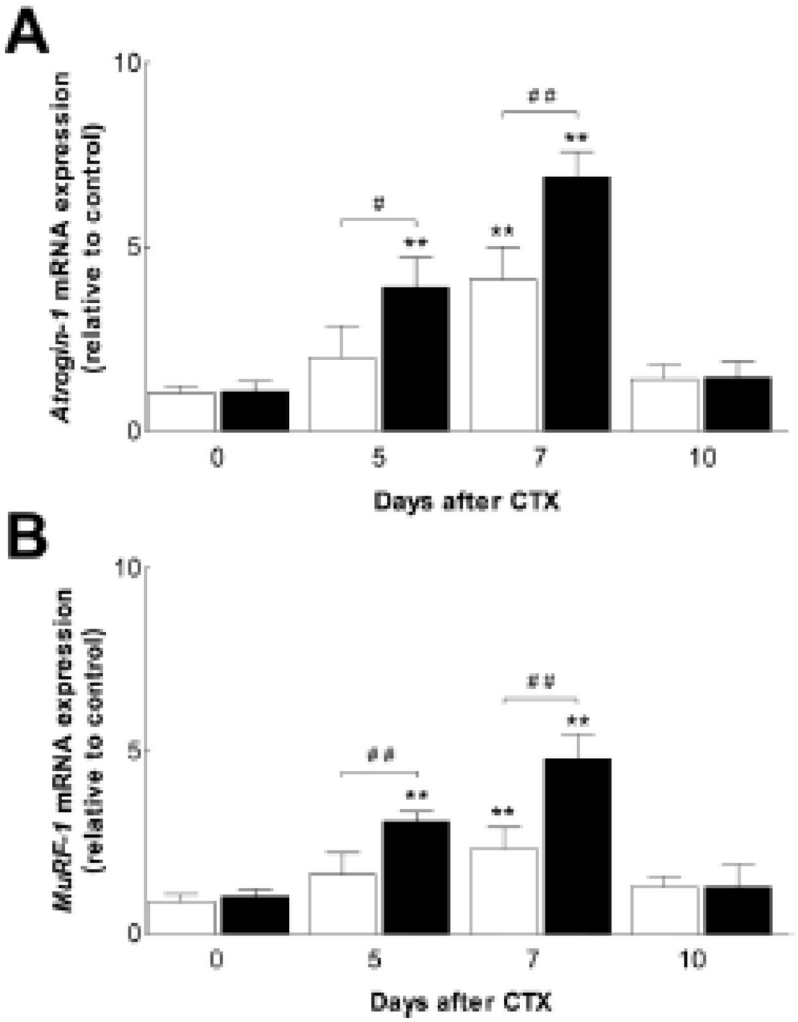

Fig. 8.

Atrogin-1 (A) and *MuRF-1* (B) mRNA expression at days 5, 7 and 10 of skeletal muscle regeneration in $Neu1^{+/+}$ (white bars) and $Neu1^{-/-}$ (black bars) TA muscles. $^{**}p<0.05$ indicates differences between gene expression of CTX-injured muscles and untreated control muscle for each genotype (day 0); $\#p<0.05$ and $\#\#p<0.01$ indicate differences between gene expression in $Neu1^{-/-}$ and $Neu1^{+/+}$ muscles on the same day of regeneration; Mann-Whitney test (n=5).

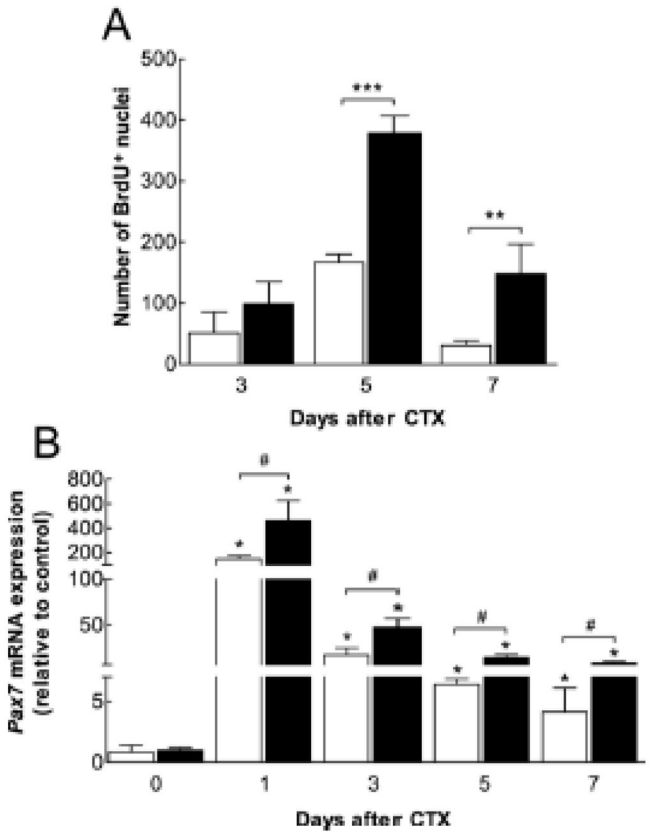

Fig. 9.

Cell proliferation during the early stages of muscle regeneration after CTX-induced injury (n=5). (A) *Neu1*$^{-/-}$ muscles (black bars) had more BrdU^{+} nuclei than did *Neu1*$^{+/+}$ muscles (white bars), indicating an elevated proliferative response. ***p <0.01* and ****p <0.001* indicate differences between *Neu1*$^{-/-}$ muscle and *Neu1*$^{+/+}$ muscle on the same day of regeneration; two-way ANOVA with Bonferroni post-test. (B) *Pax7* mRNA expression was elevated in both genotypes throughout regeneration. **p<0.05* indicates differences between the levels of *Pax7* expression and that of untreated control muscle (day 0); *#p <0.05* indicates differences between the levels of *Pax7* expression in *Neu1*$^{-/-}$ muscle and that in the *Neu1*$^{+/+}$ muscle on the same day of regeneration; Mann-Whitney test (n=5).

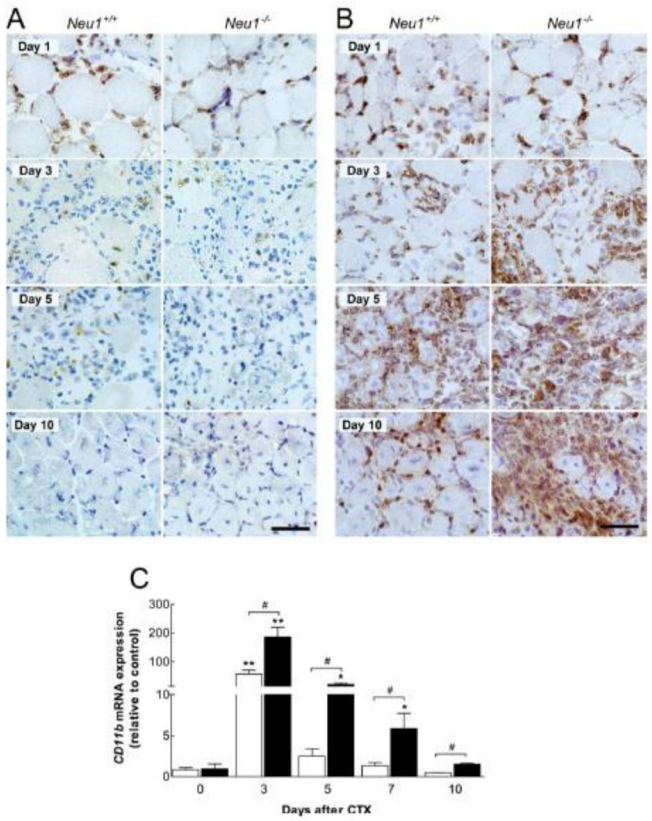

Fig. 10.

Inflammation during muscle regeneration in *Neu1*$^{+/+}$ and *Neu1*$^{-/-}$ mice (n=5). Immunohistochemical staining for neutrophils (A) and macrophages (B) shows discrepancies between the genotypes, as confirmed by *CD11b* mRNA expression analysis in *Neu1*$^{+/+}$ (white bars) and *Neu1*$^{-/-}$ (black bars) muscle (C). Scale bar = 40μm and applies to all images. *$p < 0.05$ and **$p < 0.01$ indicate differences compared with the level of expression of *CD11b* in untreated control muscle (day 0); #$p < 0.05$ indicates the differences between the levels of *CD11b* expression in *Neu1*$^{-/-}$ and *Neu1*$^{+/+}$ muscle on the same day of regeneration; Mann-Whitney test.